Magnetic state in the quasi-two-dimensional organic conductor λ-$(BEST)_2FeCl_4$ and the path of π-d interaction

Rikumaru Saito,[1] Youhei Iida,[1] Takuya Kobayashi,[2] Hiromi Taniguchi,[2] Noriaki Matsunaga,[1] Shuhei Fukuoka,[1] and Atsushi Kawamoto[1,*]

[1]*Department of Condensed Matter Physics, Graduate School of Science, Hokkaido University, Sapporo 060-0810, Japan*
[2]*Graduate School of Science and Engineering, Saitama University, Saitama 338-8570, Japan*

(Received 24 January 2022; accepted 29 March 2022; published 11 April 2022)

Studies of the quasi-two-dimensional organic conductors λ-$(D)_2MCl_4$ [D = donor molecules, M = Ga, Fe] have shown that λ-$(BETS)_2GaCl_4$ [BETS = bis(ethylenedithio)tetraselenafulvalene] undergoes an unconventional superconducting transition and λ-$(BETS)_2FeCl_4$ undergoes a field-induced superconducting transition. In λ-type salts, the interactions between donor molecules and $FeCl_4^-$ (π-d interactions) are important. To investigate π-d interaction, a pair of magnetic M = Fe and nonmagnetic M = Ga salts which have the same ground state in the donor layer is desired. However, no such pair has been found, and few experimental studies have considered π-d interaction paths. λ-$(BEST)_2MCl_4$ [BEST = bis(ethylenediseleno)tetrathiafulvalene] are obtained for both anions, and M = Ga salt shows an antiferromagnetic transition, but the ground state has not been analyzed in M = Fe salt. We perform x-ray diffraction, magnetic susceptibility measurement, and Mössbauer spectroscopy in λ-$(BEST)_2FeCl_4$. We find that a magnetic transition is observed at around 26 K. The λ-$(BEST)_2MCl_4$ system is a system in which both $FeCl_4^-$ and $GaCl_4^-$ salts show antiferromagnetic transitions. In addition, the ethylene motions observed at room temperature are ordered around 108 K, resulting in the establishment of the π-d interaction path between chalcogens and the anion, and low-field magnetization suggests that the π-d interaction in λ-$(BEST)_2FeCl_4$ is smaller than that in λ-$(BETS)_2FeCl_4$. Our results show that the inner chalcogen of donor molecules is important as the path of the interaction.

DOI: 10.1103/PhysRevB.105.165115

I. INTRODUCTION

Since the discovery of the first organic superconductor, $(TMTSF)_2PF_6$ (TMTSF = tetramethyltetraselenafulvalene), many quasi-one-dimensional and quasi-two-dimensional organic conductors have been investigated [1], including the quasi-two-dimensional organic conductor κ-$(BEDT\text{-}TTF)_2X$ [BEDT-TTF (ET) = bis(ethylenedithio)tetrathiafulvalene, X = monovalent anion]. In κ-type salts, two ET molecules form a dimer. One dimer has one hole, resulting in a half-filled system. The physical properties of these salts are characterized by U/W (U = on-site Coulomb repulsion, W = bandwidth) [2]. When U/W is large, the electronic state becomes a Mott insulator, and when U/W is small, it becomes a metal. The magnetic ground state of the Mott insulating phase in κ-type systems is an antiferromagnetic (AFM) state, with a superconducting phase being adjacent to the AFM state in the universal phase diagram [3]. These phase diagrams show that organic conductors have similarities with copper oxides and are a strongly correlated electron system [4]. In addition, the physical properties of organic conductors have been found to depend on X substitution.

Among the quasi-two-dimensional organic conductors λ-$(D)_2MCl_4$ (D = donor molecules, M = Ga, Fe), the structures of four types of donor molecules, BETS [BETS = bis(ethylenedi-thio)tetraselenafulvalene], STF [STF = bis(ethylenedithio)diselenadithiafulvalene], ET, and BEST [BEST = bis(ethylenediseleno)tetrathiafulvalene], are shown in Fig. 1(a). Similar to κ-type salts, two donor molecules form a dimer in λ-type salts [Fig. 1(b)]. λ-$(BETS)_2GaCl_4$ undergoes a superconducting (SC) transition at around 6 K [5–7]. Thermodynamic and ^{13}C nuclear magnetic resonance (NMR) studies revealed that λ-$(BETS)_2GaCl_4$ has d-wave SC gap symmetry [8,9]. A Fulde-Ferrell-Larkin-Ovchinnikov state has been suggested near the upper critical field [6,7,10,11]. In contrast, λ-$(BETS)_2FeCl_4$, which contains magnetic anions of $FeCl_4^-$ with $3d$ spins ($S = 5/2$), is the first organic material to show magnetic-field-induced superconductivity explained by the Jaccarino-Peter mechanism [12–14]. Application of an external field parallel to the conducting layers results in the alignment of Fe moments along the external field, with an internal field generated on π electrons by π-d interaction. The magnetic field on the π electrons is canceled out by the negative value of the exchange interaction $J_{\pi d}$, resulting in the emergence of superconductivity.

At zero field, this compound undergoes a metal-insulator (MI) transition at around 8 K [5]. This compound also undergoes an AFM transition at almost the same temperature, with magnetic anisotropy emerging at low temperature [15]. Evaluation of the temperature dependence of specific heat revealed a Schottky-type broad hump below the MI transition temperature likely due to the $3d$ spin degrees of freedom [16,17]. This finding indicates that the π-spin system becomes

*atkawa@sci.phys.hokudai.ac.jp

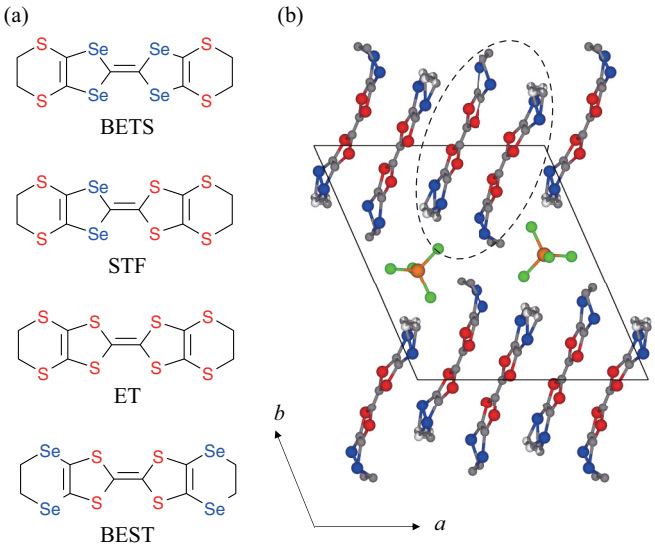

FIG. 1. (a) Donor molecular structures of BETS, STF, ET, and BEST. (b) Crystal structure of λ-$(BEST)_2FeCl_4$ at room temperature. The dimer is surrounded by a dashed curve.

an AFM long-range-ordered state at $T_{AFM} = 8.3$ K, while the 3*d* spin system remains paramagnetic. This magnetic anomaly could be explained by using a π-ordering model [17]. Below the MI transition temperature, the π electrons are localized, followed by the emergence of long-range-ordered π electrons. The alternating internal field is generated on the 3*d* electrons with the π-*d* interaction. When the external field is small, the exchange field by π-*d* interaction from AFM long-range-ordered π electrons is dominant, resulting in the AFM structure of π electrons appearing in *d* electrons. The π-*d* interaction is essential not only in high magnetic field but also in zero or small magnetic fields. In the π-ordering model, the same AFM structure in donor molecules is expected.

Although λ-$(BETS)_2GaCl_4$ and λ-$(BETS)_2FeCl_4$ have almost the same lattice constants, their ground state differs significantly. Thus λ-$(BETS)_2GaCl_4$ cannot be used as a reference system for λ-$(BETS)_2FeCl_4$, including nonmagnetic anions. Hence λ-type $FeCl_4^-$ and $GaCl_4^-$ salts with the same ground state have been explored. Unlike λ-$(BETS)_2FeCl_4$, λ-$(STF)_2FeCl_4$ is insulating in the entire temperature range, with only magnetic transition occurring [18]. The AFM transition in donor molecules at 16 K was confirmed by ^{13}C NMR [19]. Although λ-$(STF)_2GaCl_4$ is also insulating at all temperatures, no magnetic transition has been observed [20].

ET and BEST salts are also on the negative-pressure side of STF salts and insulators at all temperatures [21,22]. Recently, it was reported that λ-$(BEST)_2GaCl_4$ undergoes an AFM transition at 22 K, and the preparation of λ-$(BEST)_2FeCl_4$ has already been reported [22,23]. However, λ-$(ET)_2FeCl_4$ has not been reported, whereas λ-$(ET)_2GaCl_4$ undergoes the AFM transition at 13 K [24]. BEST salts would be good candidates for a systematic study of π-*d* interaction in the λ system.

Although molecular orbital (MO) calculations take these interactions into account [25], few experimental studies have considered these interaction paths [26]. The interaction is expected to be an exchange interaction through the Cl atom. However, the ethylene motion of the donor molecule, which is a fatal characteristic of the ethylene-dithio and ethylene-diseleno group, modulates the MCl_4^{-1} anion [27] and may hinder the π-*d* interaction. Hence how to freeze the ethylene motion at low temperature is important in the formation of π-*d* interaction. Comparisons of λ-$(BEST)_2FeCl_4$ with λ-$(BETS)_2FeCl_4$ can provide the information of the π-*d* interaction path because BEST has a structure in which the inner chalcogen, Se, and the outer chalcogen, S, in BETS molecules are interchanged. The present study therefore utilized x-ray diffraction (XRD), measurements of resistivity, and Mössbauer spectroscopy and magnetic susceptibility to determine the ground state of λ-$(BEST)_2FeCl_4$ and the π-*d* interaction path.

II. EXPERIMENTS

Single crystals of λ-$(BEST)_2FeCl_4$ were prepared by electrochemical oxidation of BEST in a solution of the tetrabutylammonium (TBA) salt of $FeCl_4^-$ in chlorobenzene. The resulting samples were black needlelike crystals, with a length corresponding to the *c* axis. No polymorphisms have been detected. XRD was performed using Mo-K_α radiation ($\lambda = 0.710\ 73$ Å) with a Bruker Apex II Ultra diffractometer equipped with a CCD area detector at the Comprehensive Analysis Center for Science, Saitama University, Japan. The x-ray data were collected from room temperature down to 108 K. Electrical resistivity was measured using the dc four-terminal method from room temperature to around 90 K. Gold wires 10 μm in diameter were attached to the sample using carbon paste. An electric current was applied parallel to the *c* axis. Magnetic susceptibility was measured using a magnetic property measurement system (MPMS) superconducting quantum interference device (SQUID) magnetometer (Quantum Design). Five single crystals (0.1756 mg) directionally aligned along the *c* axis were measured. External magnetic fields were applied parallel and perpendicular to the *c* axis. The crystals for Mössbauer measurement were prepared by electrochemical oxidation of BEST in the chlorobenzene solution with 96% ^{57}Fe-enriched TBA-$FeCl_4$. Samples weighing 35 mg were wrapped in Fe-free Al foil and attached to a He gas flow cryostat. ^{57}Co was used as a source of the γ ray. Mössbauer measurements were in constant acceleration mode at temperatures ranging from 4.4 to 50 K. Velocity was calibrated using α-Fe.

III. RESULTS AND DISCUSSION

A. X-ray diffraction

Crystals are identified by XRD at room temperature. Table I shows the lattice constants of λ-$(D)_2FeCl_4$ (D = BETS, STF, and BEST) to compare our results with those of previous studies [5,20,22]. The cell volumes of λ-$(D)_2FeCl_4$ are summarized with isostructural λ-$(D)_2GaCl_4$ in Fig. 2. λ-type salts have almost the same lattice constants even if the anions are $GaCl_4^-$ or $FeCl_4^-$. Because the atomic radius of Se is larger than that of S, the cell volumes of ET, STF, and BETS salts positively correlate with the amount of Se. The BEST molecule has the same amount of Se as the BETS molecule, whereas the cell volume of the BEST salt is larger than that

TABLE I. Lattice constants of λ-$(D)_2FeCl_4$ (D = BETS, STF, and BEST) at room temperature.

	λ-BETS	λ-STF	λ-BEST	λ-BEST
a (Å)	16.164(3)	16.238(7)	16.399(5)	16.382(3)
b (Å)	18.538(3)	18.28(1)	18.178(5)	18.160(3)
c (Å)	6.593(1)	6.574(3)	6.725(2)	6.7104(11)
α (deg)	98.40(1)	98.43(6)	97.185(3)	97.146(2)
β (deg)	96.67(1)	96.92(5)	97.797(3)	97.780(2)
γ (deg)	112.52(1)	112.37(4)	112.230(3)	112.238(2)
V (Å^3)	1773.0(5)	1751(2)	1804.1(9)	1796.9(5)
Ref.	[5]	[20]	[22]	This paper

of the BETS salt. This correlation indicates that the BEST salt could be on the negative-pressure side of the BETS salt.

The paths of π-d interactions in λ-$(D)_2FeCl_4$ could be discussed by focusing on the motions of the ethylene group and resulting displacement of $FeCl_4^-$. An Oak Ridge Thermal Ellipsoid Plot (ORTEP) drawing of the composite diagram around the anion at room temperature shows that the anion is surrounded by four molecules of crystallographically independent A (A′) and B (B′) molecules (Fig. 3). One side of the ethylene groups in the A and B molecules is disordered with the ethylene motion, and the ethylene motion modulates the anion, suggesting that significant thermal vibrations prevent the path between donor molecules and anions from being made.

XRD at low temperatures is therefore performed to determine whether the motions of ethylene groups are frozen. Table II shows the crystallographic data at 250, 200, 150, and 108 K. As shown in Fig. 4, the cell volume decreases with decreasing temperature.

An ORTEP drawing at 108 K shows that the ethylene motions of the B (B′) molecule are ordered, whereas those of the A (A′) molecule are still disordered (Fig. 5). Figure 6 shows the temperature dependence of the equivalent isotropic atomic displacement parameter, U_{eq}, which is the mean value of the principal values of the atomic displacement tensor. With decreasing temperature, U_{eq} of Cl atoms decreases, and at

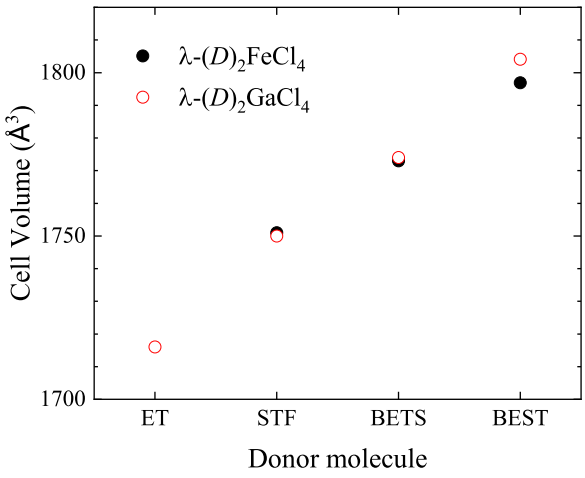

FIG. 2. Relationship between the cell volume of λ-type salts at room temperature.

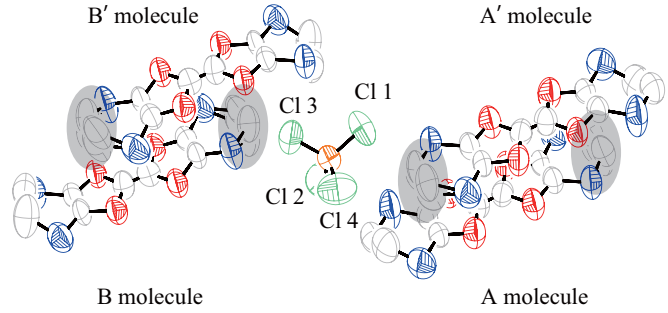

FIG. 3. ORTEP drawing of λ-$(BEST)_2FeCl_4$ at room temperature. Disordered ethylene groups are shaded in gray. The occupancies of the staggered A (A′) and B (B′) molecules are 63 and 84%, respectively. The A′ (B′) molecule is equivalent to the A (B) molecule by inversion symmetry.

108 K, U_{eq} is approximately 1/3 of that at room temperature, indicating that the displacement of Cl atoms is almost suppressed at 108 K. The ordering of the ethylene group suggests that the anion motion is suppressed by the freezing of ethylene motions. Thus the shortest distances of d_1 and d_2 from the chalcogens in ordered B (B′) molecules to the Cl atom are realized, suggesting the formation of interaction paths between donor molecules and anions. Indeed, ^{69,71}Ga NMR in isostructural λ-$(BETS)_2GaCl_4$ revealed that Bloembergen-Purcell-Pound-type molecular motion was observed at room temperature and frozen at around 100 K [27].

The short distances from the inner and outer chalcogens to the Cl atom at 108 K in BEST and BETS salts are listed in Table III. The Se (outer chalcogen)–Cl distance in λ-$(BEST)_2FeCl_4$, 3.2421(8) Å, is much shorter than the Se (inner chalcogen)–Cl distance in λ-$(BETS)_2FeCl_4$ and the van der Waals radius of 3.65 Å. Thus, if the outer chalcogen atoms are important for the π-d interaction path, the π-d interaction would be higher in λ-$(BEST)_2FeCl_4$. In contrast, if the inner chalcogen atoms are essential, then the π-d interaction would be higher in λ-$(BETS)_2FeCl_4$.

B. Resistivity

To check the semiconducting behavior, we measure the electrical resistivity. Figure 7 shows the temperature dependence of the electrical resistivity of λ-$(BEST)_2FeCl_4$ down to around 90 K at ambient pressure measured by several excitation currents. Due to the high resistance, the resistivity has been measured down to 200 K in previous studies. The resistivity is found to increase with decreasing temperature, consistent with previous findings [22]. The resistivity for the entire temperature range could be explained using the equation $\rho = A\exp(E_a/k_BT)$, where ρ, A, and E_a represent the resistivity, a constant, and the activation energy, respectively. From the fitting, we obtain $\sigma(\mathrm{RT}) = 1/\rho(\mathrm{RT}) \simeq 0.2$ S/cm and $E_a \simeq 0.08$ eV (≃930 K). The activation energy is slightly larger than the previous results of $\sigma(\mathrm{RT}) = 0.1$ S/cm and $E_a = 0.13$ eV and comparable to E_a for λ-$(STF)_2FeCl_4$ = 0.10 eV [18,22].

TABLE II. Crystallographic data of λ-$(BEST)_2FeCl_4$ at low temperatures. CCDC, Cambridge Crystallographic Data Centre; GOF, goodness of fit.

T (K)	108	150	200	250
Chemical formula	$C_{20}H_{16}FeCl_4S_8Se_8$			
Space group	$P\bar{1}$			
a (Å)	16.1204(17)	16.1613(18)	16.233(2)	16.305(2)
b (Å)	18.0522(19)	18.072(2)	18.111(2)	18.135(3)
c (Å)	6.6442(7)	6.6568(7)	6.6770(8)	6.6938(10)
α (deg)	97.4500(10)	97.3620(10)	97.277(2)	97.209(2)
β (deg)	96.9640(10)	97.1240(10)	97.322(2)	97.547(2)
γ (deg)	111.8550(10)	111.9340(10)	112.0350(10)	112.130(2)
V (Å^3)	1749.0(3)	1757.2(3)	1772.0(4)	1784.4(5)
D_{calc} (g/cm^3)	2.549	2.537	2.515	2.498
μ (cm^{-1})	9.557	9.513	9.433	9.368
F_{000}	1260	1260	1260	1260
θ maximum	29.106	29.159	27.491	25.234
Number of unique reflections	8558	8594	8056	6401
R_{int}	0.0306	0.0358	0.0434	0.0483
R_1 $[I > 2\sigma(I)]$[a]	0.0268	0.0293	0.0328	0.0346
wR_2 (all data)[b]	0.0559	0.0631	0.0731	0.0829
GOF	0.999	0.993	1.034	1.025
CCDC No.	2117595	2117596	2117597	2117598
Occupancy of staggered A (A′) molecule (%)	82	75	70	66

[a] $R_1 = \sum ||F_0| - |F_c|| / \sum |F_0|$.
[b] $wR_2 = [\sum w(|F_0| - |F_c|)^2 / \sum w|F_0|^2]^{1/2}$.

C. Magnetic susceptibility

Figure 8 shows the temperature dependence of the magnetic susceptibility from 100 to 2 K at 5 T perpendicular and parallel to the c axis. The magnetic susceptibility increases with decreasing temperature in both directions. Curie-Weiss behaviors are observed in both directions without magnetic anisotropy, and no magnetic transition is observed down to 2 K. The inset shows the Curie-Weiss plots of magnetic susceptibility. These data could be fitted using the Curie-Weiss model, with $1/\chi = T/C + T_W/C$, where χ, C, and T_W are the magnetic susceptibility, the Curie constant, and the Weiss temperature, respectively. In a paramagnetic state, the C and T_W of the salt were estimated to be ≃4.4 (emu K)/mole and approximately equal to −7.4 K, respectively, in the temperature range above 30 K. The Curie constant using $S = 5/2$ system is 4.4 (emu K)/mole, indicating that the $3d$ spins of Fe^{3+} are most responsible for magnetic susceptibility. Moreover, our finding that the Weiss temperature is negative suggests an antiferromagnetic interaction between the $3d$ spins as in λ-$(BETS)_2FeCl_4$.

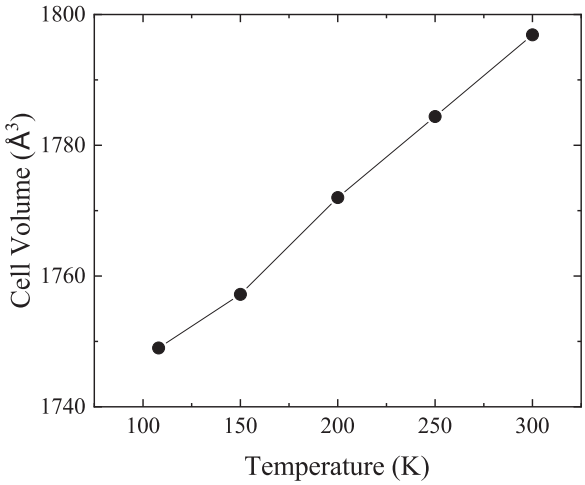

FIG. 4. Temperature dependence of cell volume of λ-$(BEST)_2FeCl_4$.

D. Mössbauer spectroscopy

Figure 9 shows Mössbauer spectra measured at several temperatures. A sharp singlet peak is observed above 26 K, indicating that the $3d$ electrons are paramagnetic. The data are fitted using Lorentzian functions, with the isomer and quadrupole shifts fixed at 0.3 and 0.2 mm/s, respectively, which are typical values for high-spin Fe^{3+} and tetrahedral

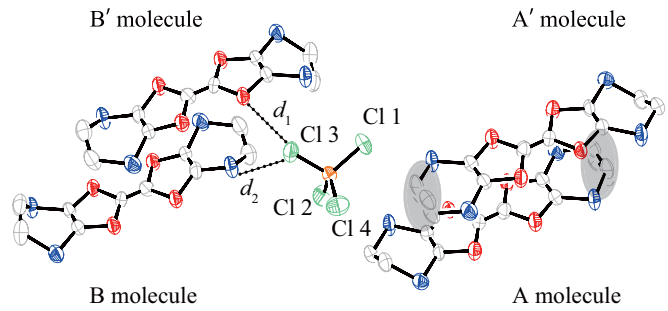

FIG. 5. ORTEP drawing of λ-$(BEST)_2FeCl_4$ at 108 K. d_1 and d_2 represent the shortest distances from the inner and outer chalcogens to the Cl atom, respectively. Disordered ethylene groups are shaded in gray.

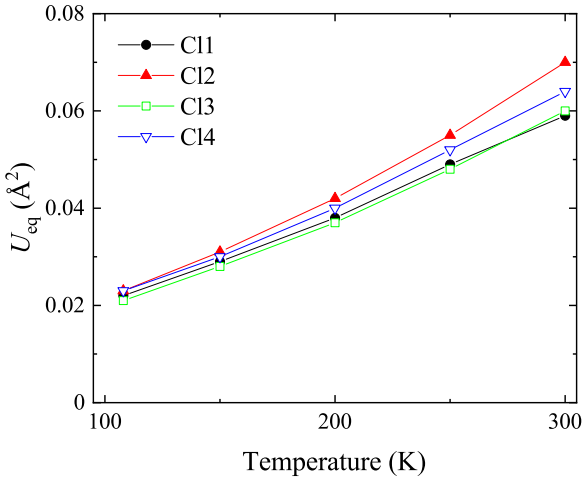

FIG. 6. Temperature dependence of the equivalent isotropic atomic displacement parameters. Cl 1, Cl 2, Cl 3, and Cl 4 correspond to the labels shown in Fig. 5.

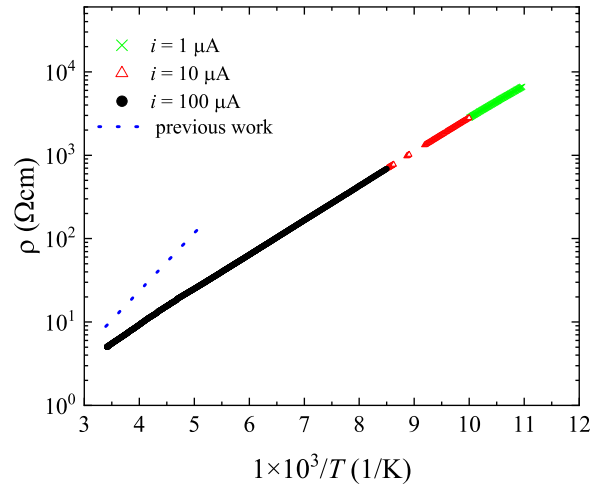

FIG. 7. Temperature dependence of the electrical resistivity of λ-$(BEST)_2FeCl_4$ at ambient pressure. The dotted line represents the data from a previous report [22].

$FeCl_4^-$. At 26 K, the broadening of the spectrum is observed, and the data could no longer be fitted using a single Lorentzian function, indicating the development of hyperfine fields at the Fe sites. Below 26 K, the singlet peak gradually splits into sextet peaks and a residual central singlet peak, enabling the data to be fitted with a sextet and a residual singlet peak. The residual singlet peak and its gradual disappearance with decreasing temperature are characteristics which have been already observed in BETS and STF salts [28,29].

Figure 10 shows the temperature dependence of the hyperfine fields of λ-$(D)_2FeCl_4$ (D = BETS, STF, and BEST). Hyperfine fields start to develop in the BEST salt at 26 K, but their magnitudes remain almost unchanged down to 16 K. Below 16 K, the hyperfine fields of the BEST salt approach the fields of the BETS and STF salts. At 4.4 K, the hyperfine field is about 40 T, close to the saturation value of 45 T for $FeCl_3$ [30].

The multistep development of the hyperfine fields, including the absence of any anomalies in magnetic susceptibility, was almost identical to that of λ-$(STF)_2FeCl_4$ except for the temperature at which the hyperfine fields started to develop [29]. Considering that the temperature in λ-$(STF)_2FeCl_4$ corresponded to the AFM transition temperature in the donor layer [19], λ-$(BEST)_2FeCl_4$ undergoes a magnetic transition at around 26 K in the donor layer. Because λ-$(BEST)_2GaCl_4$ shows an AFM transition at 22 K, as confirmed by ^{13}C NMR [23], both the $FeCl_4$ and $GaCl_4$ compounds of the BEST salts in the λ-type family show an AFM transition. To determine the accurate transition temperature and confirm the AFM transition in donor layers, ^{13}C NMR measurements on λ-$(BEST)_2FeCl_4$ are desired.

TABLE III. Distances between the inner chalcogen and Cl (d_1) and between the outer chalcogen and Cl (d_2) of λ-$(BEST)_2FeCl_4$ at 108 K and λ-$(BETS)_2FeCl_4$ at 100 K. d_1 and d_2 are defined in Fig. 5.

	d_1 (Å)	d_2 (Å)	Ref.
λ-$(BEST)_2FeCl_4$	3.5678(13) (S-Cl)	3.2421(8) (Se-Cl)	This paper
λ-$(BETS)_2FeCl_4$	3.4691(10) (Se-Cl)	3.3855(10) (S-Cl)	[26]

E. Magnetic susceptibility under low magnetic fields

In λ-$(BETS)_2FeCl_4$ and λ-$(STF)_2FeCl_4$, an anisotropy of magnetic susceptibility is present at low magnetic fields below 8 K [15,18]. In both salts, application of the external field parallel to the c axis reduced magnetic susceptibility at 2 K to about half that at 8 K. In contrast, susceptibility increased with decreasing temperature when a weak external field was applied perpendicular to the c axis. When the external field was small, the exchange field by π-d interaction from AFM

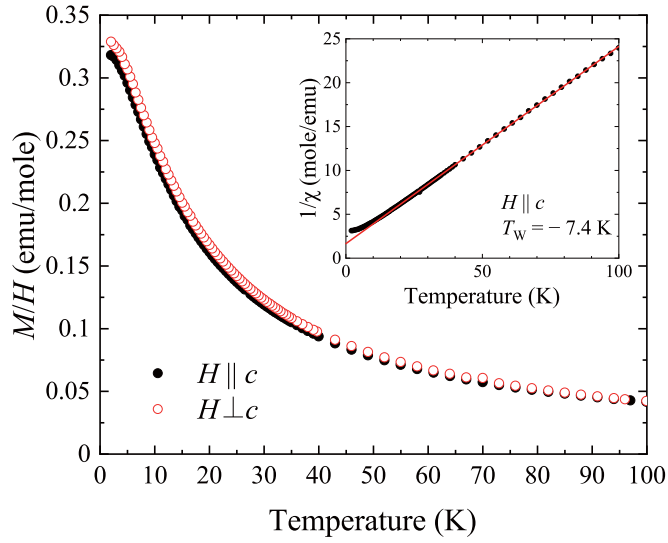

FIG. 8. Temperature dependence of the magnetic susceptibility of λ-$(BEST)_2FeCl_4$ at 5 T. External fields are applied parallel and perpendicular to the c axis. The inset shows the Curie-Weiss plots of magnetic susceptibility. The Curie constant C and the Weiss temperature T_W are estimated to be 4.4 (emu K)/mole and 7.4 K, respectively.

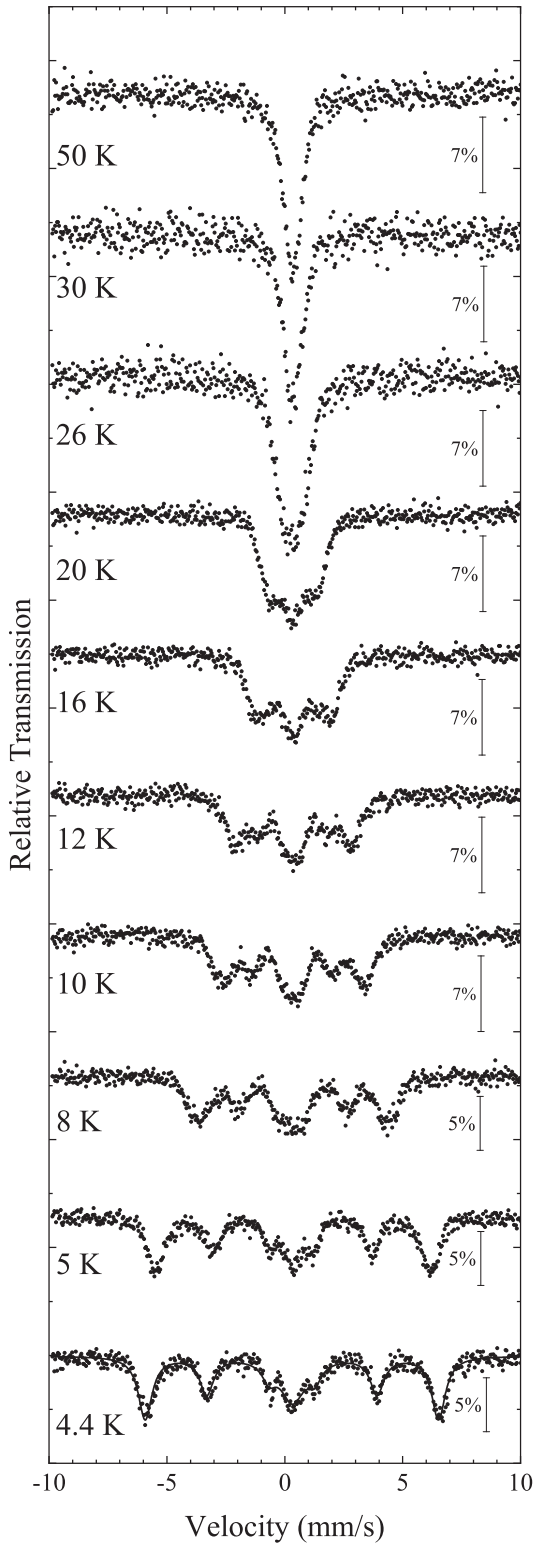

FIG. 9. Mössbauer spectra of λ-$(BEST)_2FeCl_4$ at several temperatures. The black curve is the fitting line.

long-range-ordered π electrons was dominant. The AFM structure of π electrons influences the magnetism of d electrons. Thus the c axis corresponds to the easy axis of the AFM structure in the donor layer. To investigate the anisotropy as observed in BETS and STF salts [15,18], the magnetic

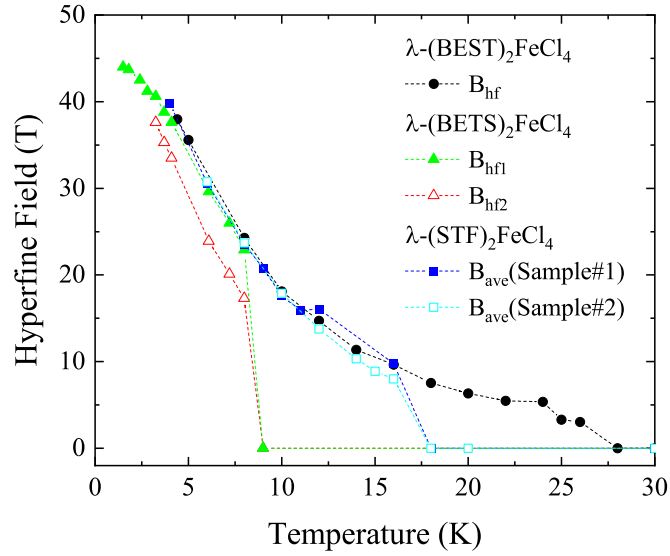

FIG. 10. Temperature dependence of the hyperfine fields of λ-$(D)_2FeCl_4$; D = BETS [28] and STF [29].

susceptibility of λ-$(BEST)_2FeCl_4$ is measured at 0.1 T. Figure 11 shows the temperature dependence of the magnetic susceptibility of λ-$(BEST)_2FeCl_4$ from 35 to 2 K in response to low external magnetic fields applied parallel and perpendicular to the c axis. Above 7 K, the magnetic suscepti-

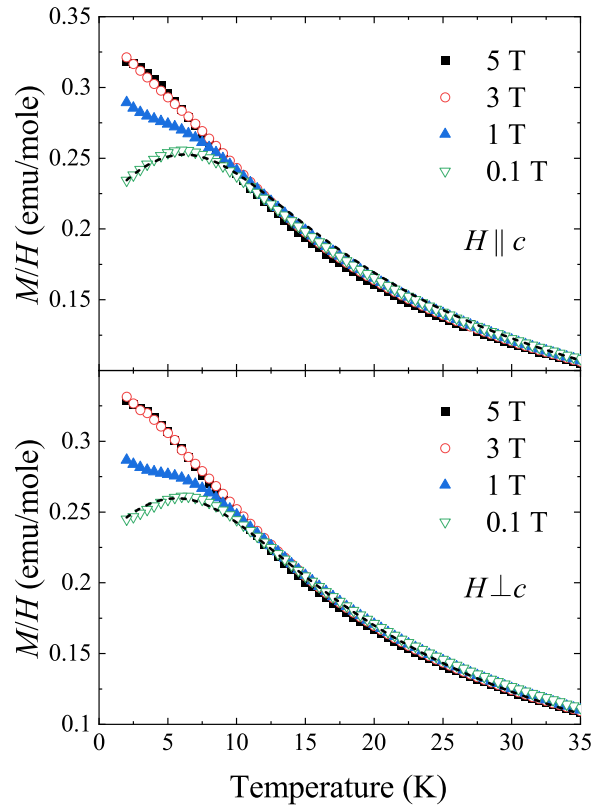

FIG. 11. Temperature dependence of the magnetic susceptibility of λ-$(BEST)_2FeCl_4$ in response to external fields perpendicular and parallel to the c axis. The dashed curve is the fitting line calculated on the basis of the π-ordering model.

bility increases with decreasing temperature in both directions without anisotropy. Below 7 K, the magnetic susceptibility decreases with decreasing temperature in both directions at 0.1 T, with weak anisotropy. The anisotropy of BETS, STF, and BEST salts disappeared when the magnetic field was increased.

Considering the π-ordering model, the π electrons of donor molecules are localized, followed by the emergence of long-range-ordered π electrons. Therefore λ-$(BETS)_2FeCl_4$ is metallic above the MI transition temperature, but at low temperatures, where an anisotropy of magnetic susceptibility appears, BETS, STF, and BEST salts are all insulators, and the characteristic shoulder in these magnetic susceptibility curves could be explained by the π-ordering model with the internal field $H_{\rm int}$ and the angle between the c axis and the easy axis θ [17,18]. We can get the parameters of $H_{\rm int} = 5.6$ T and $\theta = 45^\circ$, suggesting that the easy axis is tilted perpendicular to the c axis compared with $\theta = 25^\circ$ in BETS salt and $\theta = 33^\circ$ in STF salt. $H_{\rm int}$ is comparable to that of STF salt ($H_{\rm int} = 4.7$ T) and BETS salt ($H_{\rm int} = 4$ T), reflecting the almost hyperfine fields below 8 K in Mössbauer measurement.

The magnetic susceptibilities of λ-$(BETS)_2FeBr_xCl_{4-x}$ with several x values have been measured [31]. The replacement of Cl by Br weakened the coupling between the π and d electrons, with the ground state classified into three phases depending on the Br content. In phase I with $x < 0.2$, the π-d interaction was strong, and distinctive magnetic anisotropy was observed. Application of an external field parallel to the c axis resulted in a significant reduction in magnetic susceptibility. Magnetic anisotropy was also observed in phase III with $0.6 < x < 0.8$, characterized by decoupling of π-d electron systems [31]. Application of an external field perpendicular to the c axis resulted in a decrease in magnetic susceptibility in the same direction, suggesting that the easy axis was changed from the axis parallel to the c axis to that perpendicular to the c axis.

In phase II, which is intermediate between the above two phases, with $0.3 < x < 0.5$, the π-d electron system tended to be decoupled. Magnetic susceptibility slightly decreased in both directions, similar to λ-$(BEST)_2FeCl_4$.

Increases in the Br-to-Cl ratio were accompanied by weakening of the π-d interactions. Indeed, the Weiss temperature of λ-$(BETS)_2FeBr_xCl_{4-x}$ decreased from 15 K at $x = 0$ to 5 K at $x = 0.8$ in λ-$(BETS)_2FeBr_xCl_{4-x}$. Based on its magnetization behavior and the Weiss temperature of λ-$(BEST)_2FeCl_4$, −7.4 K, being almost half of λ-$(BETS)_2FeCl_4$, λ-$(BEST)_2FeCl_4$ corresponds to phase II in λ-$(BETS)_2FeBr_xCl_{4-x}$, indicating that the π-d interaction in λ-$(BEST)_2FeCl_4$ is weaker than that of λ-$(BETS)_2FeCl_4$.

Generally, the direction of the easy axis could be correlated with the structural and electronic properties. However, the three salts are isostructural and insulators at low temperatures. In fact, the magnetization, specific heat, and Mössbauer spectra of STF salt at low temperatures show the same behavior as those of BETS salt [17,18,28,29,32]. Since the number of selenium atoms in the STF molecule is reduced from that in the BETS molecule, the π-d interaction of λ-$(STF)_2FeCl_4$ is expected to be smaller than that of λ-$(BETS)_2FeCl_4$. Indeed, the angle between the c axis and the easy axis ($\theta = 33^\circ$) in λ-$(STF)_2FeCl_4$ was more tilted than $\theta = 25^\circ$ in λ-$(BETS)_2FeCl_4$ as in λ-$(BETS)_2FeBr_xCl_{4-x}$. The results could suggest that the correlation between the strength of the π-d interaction and the direction of the easy axis is expected to be a common characteristic in λ-type salts.

XRD results show that λ-$(BEST)_2FeCl_4$ has significantly shorter Se-Cl contact, suggesting that its π-d interactions are enhanced if the outer chalcogen is essential to the path of interaction. However, the π-d interaction of λ-$(BEST)_2FeCl_4$ is weaker than that of the BETS salt, indicating that the inner chalcogen is essential to the path of interaction.

IV. CONCLUSION

XRD results show that the ethylene groups are disordered at room temperature, although one of these groups becomes ordered at low temperature suggesting the formation of the short chalcogen-Cl contacts without ethylene disorder.

Measurements of magnetic susceptibility in external fields of 5 T show that this compound exhibits Curie-Weiss behavior, with $S = 5/2$ corresponding to Fe^{3+}. Based on the Curie-Weiss plot, the Weiss temperature is estimated to be −7.4 K.

Mössbauer measurements show the development of hyperfine fields similar to those of STF salts, with a magnetic transition temperature of 26 K in the donor layer. Because λ-$(BEST)_2GaCl_4$ shows an AFM transition at 22 K, as confirmed by ^{13}C NMR, BEST salts are λ-type $FeCl_4^-$ and $GaCl_4^-$ salts which show an AFM transition. We obtained a pair of magnetic M = Fe and nonmagnetic M = Ga salts which have same ground state, and it is interesting to investigate whether the AFM structure of λ-$(BEST)_2FeCl_4$ is the same as the AFM structure of λ-$(BEST)_2GaCl_4$. We are now performing ^{13}C NMR measurements on λ-$(BEST)_2FeCl_4$ in order to investigate the AFM structure of λ-$(BEST)_2FeCl_4$.

The magnetic susceptibility of both BETS and STF salts was shown to decrease by about 50% when a low magnetic field was applied parallel to the c axis. The magnetic susceptibility of the BEST salt slightly decreases by about 30% in both directions. This magnetic susceptibility behavior is very similar to that of phase II of λ-$(BETS)_2FeBr_xCl_{4-x}$, indicating that the π-d interaction is weaker in BEST than in BETS salts. The distances between chalcogen and Cl atoms in the anion indicate that the inner chalcogen is essential for the path of the π-d interaction.

ACKNOWLEDGMENTS

We thank A. Ito for the magnetic susceptibility measurements. This work was partially supported by Hokkaido University (Japan), Global Facility Center (GFC), Advanced Physical Property Open Unit (APPOU), funded by MEXT (Japan) under "Support Program for Implementation of New Equipment Sharing System" (JPMXS0420100318). This work was also partially supported by Japan Society for the Promotion of Science KAKENHI Grants No. 20K14401, No. 19K03758, No. 21K03438, and No. 19K0375809.

[1] D. Jèrome, A. Mazaud, M. Ribault, and K. Bechgaard, J. Phys. Lett. **41**, 95 (1980).
[2] K. Kanoda, Hyperfine Interact. **104**, 235 (1997).
[3] A. Kawamoto, H. Taniguchi, and K. Kanoda, J. Am. Chem. Soc. **120**, 10984 (1998).
[4] R. H. McKenzie, Science **278**, 820 (1997).
[5] A. Kobayashi, T. Udagawa, H. Tomita, T. Naito, and H. Kobayashi, Chem. Lett. **22**, 2179 (1993).
[6] M. A. Tanatar, T. Ishiguro, H. Tanaka, and H. Kobayashi, Phys. Rev. B **66**, 134503 (2002).
[7] S. Uji, K. Kodama, K. Sugii, T. Terashima, T. Yamaguchi, N. Kurita, S. Tsuchiya, T. Konoike, M. Kimata, A. Kobayashi, B. Zhou, and H. Kobayashi, J. Phys. Soc. Jpn. **84**, 104709 (2015).
[8] S. Imajo, S. Yamashita, H. Akutsu, H. Kumagai, T. Kobayashi, A. Kawamoto, and Y. Nakazawa, J. Phys. Soc. Jpn. **88**, 023702 (2019).
[9] T. Kobayashi, H. Taniguchi, A. Ohnuma, and A. Kawamoto, Phys. Rev. B **102**, 121106(R) (2020).
[10] W. A. Coniglio, L. E. Winter, K. Cho, C. C. Agosta, B. Fravel, and L. K. Montgomery, Phys. Rev. B **83**, 224507 (2011).
[11] S. Imajo, T. Kobayashi, A. Kawamoto, K. Kindo, and Y. Nakazawa, Phys. Rev. B **103**, L220501 (2021).
[12] S. Uji, T. Shinagawa, T. Terashima, T. Yakabe, Y. Terai, M. Tokumoto, A. Kobayashi, H. Tanaka, and H. Kobayashi, Nature (London) **410**, 908 (2001).
[13] L. Balicas, J. S. Brooks, K. Storr, S. Uji, M. Tokumoto, H. Tanaka, H. Kobayashi, A. Kobayashi, V. Barzykin, and L. P. Gor'kov, Phys. Rev. Lett. **87**, 067002 (2001).
[14] V. Jaccarino and M. Peter, Phys. Rev. Lett. **9**, 290 (1962).
[15] H. Akutsu, E. Arai, and H. Kobayashi, J. Am. Chem. Soc. **119**, 12681 (1997).
[16] H. Akiba, S. Nakano, Y. Kajita, B. Zhou, A. Kobayashi, and H. Kobayashi, J. Phys. Soc. Jpn. **78**, 033601 (2009)
[17] H. Akiba, K. Nobori, K. Shimada, Y. Nishio, K. Kajita, B. Zhou, A. Kobayashi, and H. Kobayashi, J. Phys. Soc. Jpn. **80**, 063601 (2011).
[18] T. Minamidate, H. Shindo, Y. Ihara, A. Kawamoto, N. Matsunaga, and K. Nomura, Phys. Rev. B **97**, 104404 (2018).
[19] S. Fukuoka, T. Minamidate, Y. Ihara, and A. Kawamoto, Phys. Rev. B **101**, 184402 (2020).
[20] H. Mori, H. Suzuki, T. Okano, H. Moriyama, Y. Nishio, K. Kajita, M. Kodani, K. Takimiya, and T. Otsubo, J. Solid State Chem. **168**, 626 (2002).
[21] H. Mori, T. Okano, M. Kamiya, M. Haemori, H. Suzuki, S. Tanaka, Y. Nishio, K. Kajita, and H. Moriyama, Phys. C (Amsterdam) **357-360**, 103 (2001).
[22] H. B. Cui, S. Otsubo, Y. Okano, and H. Kobayashi, Chem. Lett. **34**, 254 (2005).
[23] A. Ito, T. Kobayashi, P. D. Sari, I. Watanabe, Y. Saito, A. Kawamoto, H. Tsunakawa, K. Satoh, and H. Taniguchi, arXiv:2112.05972 [cond-mat.str-el].
[24] Y. Saito, S. Fukuoka, T. Kobayashi, A. Kawamoto, and H. Mori, J. Phys. Soc. Jpn. **87**, 013707 (2018).
[25] T. Mori and M. Katsuhara, J. Phys. Soc. Jpn. **71**, 826 (2002).
[26] T. Lee, Y. Oshima, H. Cui, and R. Kato, J. Phys. Soc. Jpn. **87**, 114702 (2018).
[27] T. Kobayashi, K. Tsuji, A. Ohnuma, and A. Kawamoto, Phys. Rev. B **102**, 235131 (2020).
[28] J. C. Waerenborgh, S. Rabaca, M. Almeida, E. B. Lopes, A. Kobayashi, B. Zhou, and J. S. Brooks, Phys. Rev. B **81**, 060413(R) (2010).
[29] S. Fukuoka, M. Sawada, T. Minamidate, N. Matsunaga, K. Nomura, Y. Ihara, A. Kawamoto, Y. Doi, M. Wakeshima, and Y. Hinatsu, J. Phys. Soc. Jpn. **87**, 093705 (2018).
[30] N. N. Greenwood and T. C. Gibb, *Mössbauer Spectroscopy* (Chapman and Hall, London, 1971).
[31] H. Akutsu, K. Kato, E. Ojima, H. Kobayashi, H. Tanaka, A. Kobayashi, and P. Cassoux, Phys. Rev. B **58**, 9294 (1998).
[32] S. Fukuoka, T. Minamidate, N. Matsunaga, Y. Ihara, and A. Kawamoto, J. Phys. Soc. Jpn. **89**, 073704 (2020).